HHS Public Access

Author manuscript

J Bone Miner Res. Author manuscript; available in PMC 2019 July 01.

Published in final edited form as:

J Bone Miner Res. 2018 July ; 33(7): 1362–1375. doi:10.1002/jbmr.3422.

The deletion of *Hdac4* in mouse osteoblasts influences both catabolic and anabolic effects in bone

Teruyo Nakatani, Ph.D[1], **Tiffany Chen, D.D.S.**[1], **Joshua Johnson, M.S.**[1], **Jennifer J. Westendorf, Ph.D**[2], and **Nicola C. Partridge, Ph.D**[1]

[1]Department of Basic Science and Craniofacial Biology, New York University College of Dentistry, New York, NY 10010

[2]Department of Orthopedic Surgery, Mayo Clinic, Rochester, MN 55905

Abstract

Histone deacetylase 4 (Hdac4) is known to control chondrocyte hypertrophy and bone formation. We have previously shown that parathyroid hormone (PTH) regulates many aspects of Hdac4 function in osteoblastic cells in vitro; however, in vivo confirmation was previously precluded by pre-weaning lethality of the Hdac4 deficient mice. To analyze the function of Hdac4 in bone in mature animals, we generated mice with osteoblast lineage-specific knockout of *Hdac4* (*Hdac4*$^{ob-/-}$) by crossing transgenic mice expressing Cre recombinase under the control of a 2.3kb fragment of the Col1a1 promoter with mice bearing loxP-*Hdac4*. The *Hdac4*$^{ob-/-}$ mice survive to adulthood and developed a mild skeletal phenotype. At 12 weeks of age, they had short, irregularly-shaped and stiff tails due to smaller tail vertebrae, with almost no growth plates. The tibial growth plate zone was also thinned and *Mmp13* and *Sost* mRNAs were increased in the distal femurs of *Hdac4*$^{ob-/-}$ mice. Immunohistochemistry showed that sclerostin was elevated in *Hdac4*$^{ob-/-}$ mice, suggesting that Hdac4 inhibits its gene and protein expression. To determine the effect of PTH in these mice, hPTH (1–34) or saline were delivered for 14 days with subcutaneously implanted devices in 8-week-old female *Hdac4*$^{ob-/-}$ and wild type (*Hdac4*$^{fl/fl}$) mice. Serum CTX, a marker of bone resorption, was increased in *Hdac4*$^{ob-/-}$ mice with or without PTH treatment. Tibial cortical BV/TV, Ct.Th, and relative cortical area (RCA) were decreased in *Hdac4*$^{ob-/-}$ mice but PTH caused no further decrease in *Hdac4*$^{ob-/-}$ mice. Tibial trabecular BV/TV and thickness were not changed significantly in *Hdac4*$^{ob-/-}$ mice but decreased with PTH treatment. These results indicate that Hdac4 inhibits bone resorption and has anabolic effects via inhibiting *Mmp13* and *Sost*/sclerostin expression. Hdac4 influences cortical bone mass and thickness and knockout of *Hdac4* prevents the catabolic effect of PTH in cortical bone.

Corresponding Author: Nicola C. Partridge, Ph.D. Department of Basic Science and Craniofacial Biology, New York University College of Dentistry, 345 East 24th St. 902A, New York, NY 10010, USA, Tel.: (212) 992-7145, Fax: (212) 995-4087, ncp234@nyu.edu.

Authors' roles: Study concept and design: TN, NCP. Data collection: TN, TC, JJ. Data analysis: TN, NCP. Data interpretation: TN, JJW, NCP. Drafting manuscript: TN, JJW, NCP. Approving final version of manuscript: TN, TC, JJ, JJW, NCP. TN takes responsibility for the integrity of the data analysis.

Disclosure Statement: The authors state that they have no conflicts of interest pertaining to the work described.

Keywords

Catabolic effects of PTH; HDAC4; Osteoblasts; Sclerostin; Cortical bone

INTRODUCTION

Parathyroid hormone (PTH) is an 84-amino acid peptide that regulates calcium and phosphorous concentrations in extracellular fluids. PTH stimulates both catabolic (bone resorption) and anabolic (bone formation) events in the skeleton depending on its dose and the periodicity of its delivery. In humans, continuous elevation of serum PTH levels, as occurs in patients with primary hyperparathyroidism, has a catabolic action on bone, while intermittent daily injection is an approved anabolic therapy for the treatment of osteoporosis.[1] PTH binds to its receptor, PTH1R on osteoblasts, and modulates the expression of key genes that control bone formation, such as *Runx2*, osterix, collagen type I alpha 1 (Col1a1), and *bone sialoprotein* (BSP) as well as genes of resorption, such as *matrix metalloproteinase*-13 (*Mmp13*) and receptor activator of nuclear factor κ–B *ligand* (RankL). Zhao *et al*. showed that collagenolytic degradation was required for PTH's stimulation of serum calcium, suggesting a role for MMP13 in bone resorption.[2]

Histone deacetylases (HDACs) exert gene regulation in skeletal cells by removing acetyl groups from histones and other proteins, including transcription factors, leading ultimately to condensed chromatin, and suppression of gene transcription. Several HDACs contribute to skeletal development and bone mass maintenance.[3] HDAC4, a class IIa histone deacetylase, is expressed in osteoblasts and prehypertrophic chondrocytes. HDAC4 represses the function of the transcription factors, Runx2 and MEF2C, preventing progression of chondrocytes to hypertrophy. [4,5] HDAC4 also deacetylates Runx2, resulting in repression of its transcriptional activity and its degradation in osteoblasts.[6] Mice with global deletion of *Hdac4* (*Hdac4*$^{-/-}$) are significantly smaller than wild type mice and die within 7 days after birth.[7] This is mainly due to ectopic ossification of endochondral cartilage (premature hypertrophy of chondrocytes and, thus, mineralization), which prevents expansion of the rib cage and leads to an inability to breathe.[4] Previous work from our laboratory has shown that in osteoblastic cells (UMR 106–01), HDAC4 represses the *Mmp13* gene under basal conditions by inhibiting the activity of Runx2. *Hdac4*$^{-/-}$ mice displayed elevated expression of *Mmp13* mRNA and protein levels in hypertrophic chondrocytes and trabecular bone.[8] We also found that HDAC4 interacts with MEF2C at the *Mmp13* promoter. PTH causes dissociation of HDAC4 from both Runx2 and MEF2C in osteoblastic cells.[9] Obri *et al.* have reported that HDAC4 inhibits *RankL* expression by its actions on MEF2C.[10] However, the role of HDAC4 in osteoblasts *in vivo* is still not well understood in detail.

Sclerostin, encoded by the *Sost* gene, has been identified as a negative regulator of bone formation.[11, 12] PTH suppresses *SOST* expression in vivo and in vitro (UMR 106 cells).[13] Class IIa HDACs (HDAC4 and HDAC5) also suppress SOST expression in osteocytes. [14, 15] On the other hand, Class I HDACs 1, 2 and 3 are required for Sost expression[16] and MEF2A, C, and D positively regulate *SOST* expression in UMR 106 cells. [17]

In the present study, to define the roles of HDAC4 in osteoblasts/osteocytes and in PTH's actions on bone, we generated osteoblast-specific knockout of *Hdac4* (*Hdac4*$^{ob-/-}$) in mice. We demonstrate that HDAC4 influences cortical bone mass and thickness and conditional deletion of *Hdac4* in osteoblasts prevents the catabolic effect of PTH in cortical bone. We conclude that HDAC4 inhibits bone resorption and has an anabolic effect via inhibiting *Mmp13* and *SOST* gene expression.

Materials and Methods

Generation of osteoblast-specific Hdac4 knockout mice

All experiments using mice were performed following protocols approved by the New York University Institutional Animal Care and Use Committee (IACUC). Col2.3 1a(I)-Cre and HDAC4 floxed mice (*Hdac4*$^{fl/fl}$) were on C57Bl/6 backgrounds. To delete Hdac4 specifically in mature osteoblasts and osteocytes, Hdac4$^{fl/fl}$ mice were crossed with mice bearing the 2.3-kb fragment of the rat α1(I)–collagen promoter fused to Cre. All genotypes were determined using Direct PCR lysis reagent (Viagen Biotech, Los Angeles, CA, USA) and the primers are listed in Table 1. All mice were housed maximally at 5 per cage at 23℃ under standard conditions with a 12-hour light/12-hour dark cycle and free access to water and standard rodent chow.

Body composition analysis

Male or female *Hdac4*$^{ob-/-}$ and control (*Hdac4*$^{fl/fl}$) mice (10 mice in each group) at 10 or 12 weeks of age were anesthetized by ketamine (100 mg/kg) and xylazine (10 mg/kg) and percentage fat determined using a Lunar PIXImus densitometer (Lunar Corporation, Madison, WI).

Continuous PTH infusion

8-week-old female *Hdac4*$^{ob-/-}$ and control (*Hdac4*$^{fl/fl}$) mice (10 mice in each group) were randomly distributed to vehicle or treatment groups and infused with continuous hPTH (1–34; Bachem) at a dose of 8μg/kg BW/day or vehicle (saline) with Alzet microosmotic pumps (model 1002, Durect, CA, USA) implanted subcutaneously onto the backs at a pumping rate of 0.25 μl/h for 14 days. Some investigators were blinded during allocation, animal handling and endpoint measurements.

Histological Analysis

10-week-old female *Hdac4*$^{ob-/-}$ and control (*Hdac4*$^{fl/fl}$) mice (10 mice in each group) were anesthetized with ketamine and the following tissue samples were retrieved. Tibiae, vertebrae, femurs and tails were fixed in 4% paraformadehyde at 4°C overnight. The samples were then decalcified in 10% EDTA. Paraformaldehyde-fixed paraffin-embedded femurs and tibiae were cut as 5 μm sections, and stained with hematoxylin and eosin (H&E). Immunohistochemical analysis of sclerostin (R&D Systems) was carried out on similar sections. Briefly, deparaffinized and hydrated sections were incubated with Proteinase K Solution (20 μg/ml in TE Buffer, pH 8.0) for 20 min in a water bath at 37°C. After cooling, the sections were rinsed with PBS, the endogenous peroxidase was removed by incubating sections for 15 min at room temperature in 3% H_2O_2 in methanol. After rinsing sections in a

BSA solution (3% in PBS), blocking for 1 hour at room temperature (BSA solution containing 1% Triton and 5% FBS) was performed. Primary antibody diluted in PBS with 3% milk (goat anti-Sclerostin: 1:30) was incubated overnight at 4°C in a humidifying chamber. After three washes in PBS-BSA solution, secondary donkey anti-goat peroxidase (HRP)-conjugated antibody (Santa Cruz Biotechnology) was incubated with the sections for 1 hour at room temperature. Sections were developed using Fast 3′3′-Diaminobenzidine (Sigma-Aldrich), prepared following the manufacturer's protocol and, after washing with PBS, counterstained with hematoxylin (Sigma-Aldrich) for 1 min. Slides were mounted using Permount mounting medium (Thermo Scientific). Sclerostin-positive osteocytes were manually counted using image J.

TRAP staining of tibial bone sections

Tartrate resistant acid phosphatase (TRAP) staining was performed using the Acid Phosphatase Leukocyte kit (Sigma-Aldrich, St. Louis, MO, USA) following the manufacturer's protocol after deparaffinization and acetate buffer washing. The staining of surface osteoclasts was quantified using BIOQUANT OSTEO 2015.

Micro-computed tomography (μCT) analysis

The tibiae and vertebrae of mice (female) were fixed in 70% ethanol and prepared for high-resolution μCT (SkyScan 1172). Images were obtained using the following parameters: 60 Kv, 167 μA, pixel size of 9.7 μm, 2000×1332 matrix, 6 averages and a 0.5mm aluminum filter. Images were reconstructed using a thresholding of 0–0.065, beam hardening correction of 40, ring artefact correction of 7, and Gaussian smoothing (factor = 1). The tibial cortical analysis was performed on a region extending 50% of the bone length from the proximal end and extending 62 slices for total cortical cross -sectional bone area (Tt.Ar), cross-sectional marrow area (Ma.Ar), cortical bone (tissue) area (Ct.Ar), polar moment of inertia (MMI) and cortical thickness (Ct.Th). Relative cortical area (RCA) was defined as Ct.Ar/Tt.Ar and represented the relative amount of bone tissue in a given bone area. The trabecular analysis was performed on a region starting 25 slices from the end of the growth plate and extending 258 slices toward the distal tibia. This was examined for trabecular bone mineral density (BMD), bone volume/total volume (BV/TV), trabecular number (Tb.N), trabecular thickness (Tb.Th), and trabecular spacing (Tb.Sp). BMD was calculated as the ratio of bone mineral content (BMC, mg) to the total volume of distal metaphysis analyzed after removing (masking) marrow space grayscale variability. Caudal vertebra 17 cortical analysis was performed on a region of 150 and 70 scan slices from above the caudal growth plate for $Hdac4^{fl/fl}$ and $Hdac4^{ob-/-}$ mice, respectively. Lumbar vertebrae (L4) analysis was performed on the same circular area. The bone parameters were obtained with CtAn Version 1.5 (SkyScan).

Quantitative real-time RT-PCR

Total RNA was obtained from distal femurs using TRIzol reagent (Invitrogen, CA, USA). cDNA was synthesized from 0.1 μg of total RNA using a TaqMan reverse transcription kit (Life Technologies, USA.) with hexamer primers following the protocol described by the manufacturers. Gene expression levels were measured using SYBR Green PCR Reagent (Applied Biosystems). Primer pairs used for quantitative detection of gene expression are

listed in Table 2. The quantity of mRNA was calculated by normalizing the Ct (threshold cycle value) of specific genes to the Ct of the housekeeping gene β-actin.

Serum biomarkers

Serum was prepared by allowing the blood to clot for 15–30 min at room temperature followed by centrifugation at 2000 × g for 10 min at 4°C. CTX and P1NP (Immunodiagnostic Systems Inc.) were measured by sandwich ELISAs. All measurements were performed according to the manufacturer's instructions included with the kits.

Statistical analyses

Statistical differences were analyzed either by Student's t test or by two -way ANOVA using IBM SPSS (v22, Armonk, NY). Results are expressed as mean ± SE and a $p < 0.05$ was considered significant comparing each of the groups.

Results

Phenotype of osteoblast-specific *Hdac4* deficient mice

We confirmed the specificity of Hdac4 gene excision in the *Col2.3-Cre/Hdac4*$^{fl/fl}$ mice by PCR analysis of genomic DNA from different tissues from mature osteoblast lineage-specific, knockout (*Hdac4*$^{ob-/-}$), and the control (*Hdac4*$^{fl/fl}$) mice. Exon 4 excision (*Δ-Hdac4*) occurred in calvariae and bone from *Hdac4*$^{ob-/-}$ mice but not in *Hdac4*$^{fl/fl}$ (Fig 1A). Although the excision also seemed to occur in the heart, we confirmed that HDAC4 protein and *Hdac4* mRNA were not affected in the hearts of *Hdac4*$^{ob-/-}$ mice (Fig. 1B). *Hdac4* gene expression levels were approximately decreased by 70% in the distal femur (Fig. 1C) and *Mmp13* gene expression was increased by 40% (Fig. 1D). Thus, the establishment of mature osteoblast lineage-specific ablation of HDAC4 was confirmed in *Hdac4*$^{ob-/-}$ mice.

These mice survived to adulthood but showed a mild skeletal phenotype upon gross examination. Female *Hdac4* mutant mice were noticeably smaller and weighed around 7% less than *Hdac4*$^{fl/fl}$ mice but had similar fat percentages (Fig. 2B). There were no significant differences in body weight or fat percentage in male mice (Fig. 2A). Most striking was that all *Hdac4*$^{ob-/-}$ mice had shorter, irregularly-shaped, and stiff tails at 12 weeks of age (Fig. 2A, B). Representative μCT images of caudal vertebrae from female *Hdac4*$^{fl/fl}$ and *Hdac4*$^{ob-/-}$ mice are shown in Fig. 3A. The μCT of caudal vertebra 17 revealed low cortical bone volume (BV/TV), bone area (Ct.Th and RCA), and length compared with *Hdac4*$^{fl/fl}$ mice. On the other hand, porosity was increased in *Hdac4*$^{ob-/-}$ mice (Fig. 3B). Hematoxylin and eosin staining of caudal vertebrae showed that the tail phenotype in *Hdac4*$^{ob-/-}$ mice is due to shorter tail joints, with lesser growth plates and abnormal intervertebral discs (Fig. 3C). The lumbar intervertebral discs also seem to be deformed compared with *Hdac4*$^{fl/fl}$ mice (Fig. 3D). The μCT of lumbar vertebrae revealed that *Hdac4*$^{ob-/-}$ mice have greater Tb.Pf and lower DA compared with *Hdac4*$^{fl/fl}$ mice (Fig. 3E), suggesting that lumbar vertebral trabecular bone of *Hdac4*$^{ob-/-}$ mice is more disconnected and is weaker than *Hdac4*$^{fl/fl}$ mice. Overall, these data suggest that Hdac4 is required for caudal and lumbar vertebral bone mass and strength in mice.

HDAC4 regulates body weight and length of growth plates of long bones

To determine the role of HDAC4 in the catabolic action of PTH, 8-week-old female *Hdac4*$^{ob-/-}$ or *Hdac4*$^{fl/fl}$ mice were treated with continuous infusion of PTH for 2 weeks. Body weight was significantly decreased in *Hdac4*$^{ob-/-}$ compared to *Hdac4*$^{fl/fl}$ mice. PTH treatment induced significant body weight loss (approximately 10%) from baseline in both *Hdac4*$^{fl/fl}$ and *Hdac4*$^{ob-/-}$ mice (Figure 4A). There was no significant change in fat percentage between control and PTH-infused *Hdac4*$^{ob-/-}$ or *Hdac4*$^{fl/fl}$ mice (Figure 4B). Histological examination of tibiae showed significantly shorter tibial prehypertrophic and hypertrophic growth plate zones in *Hdac4*$^{ob-/-}$ compared to *Hdac4*$^{fl/fl}$ mice. On the other hand, continuous PTH treatment (both *Hdac4*$^{fl/fl}$ and *Hdac4*$^{ob-/-}$ mice) caused lengthening of both zones (Fig. 4C, D).

HDAC4 is required for normal accrual of cortical bone mass and for PTH's catabolic effects on cortical bone

We performed μCT analysis to determine the tibial cortical structure. *Hdac4*$^{ob-/-}$ mice exhibited decreased cortical bone volume (BV/TV), cortical thickness (Ct.Th), relative cortical area (RCA), T.Ar, B.Ar, BMD and MMI compared to *Hdac4*$^{fl/fl}$ mice. Continuous PTH treatment significantly reduced cortical BV/TV, Ct.Th, and RCA in wild-type animals. In contrast, *Hdac4*$^{ob-/-}$ mice were protected from the PTH-induced decrease in BV/TV, bone area and architecture (Figure 5A). These results indicate that HDAC4 is involved in maintenance of cortical bone mass and thickness and genetic deletion of *Hdac4* in osteoblastic cells prevents the catabolic effect of PTH in cortical bone.

Continuous PTH treatment decreased trabecular bone mass; *Hdac4* deficiency did not attenuate this decrease in trabecular bone

We observed that continuous PTH treatment significantly decreased tibial trabecular BV/TV, trabecular thickness (Tb.Th), and trabecular number (Tb.N) in *Hdac4*$^{fl/fl}$ and *Hdac4*$^{ob-/-}$ mice. On the other hand, there were no significant differences comparing *Hdac4*$^{ob-/-}$ with *Hdac4*$^{fl/fl}$ mice and *Hdac4* deficiency did not attenuate the PTH catabolic action in trabecular bone (Figure 5B). Trabecular separation (Tb. Sp) was significantly increased in *Hdac4*$^{ob-/-}$ mice and was further increased by PTH treatment in the knockout mice. These data suggest that continuous PTH increases trabecular bone loss and HDAC4 deletion does not prevent the catabolic effect of PTH in trabecular bone.

HDAC4 counteracts bone resorption

To determine the role of HDAC4 in bone resorption, we examined TRAP staining, a marker of differentiated osteoclasts in *Hdac4*$^{fl/fl}$ and *Hdac4*$^{ob-/-}$ mice (Fig. 6A). Quantitative analysis, osteoclast numbers (N.Oc/BS, n/mm) and osteoclast surface (Oc.S/BS, %) relative to bone surface were higher in *Hdac4*$^{ob-/-}$ mice compared to *Hdac4*$^{fl/fl}$ mice. Continuous PTH treatment increased these indices of osteoclastic function in both *Hdac4*$^{fl/fl}$ and *Hdac4*$^{ob-/-}$ groups (Fig. 6B, C). Serum CTX levels, a circulating bone resorption marker, were significantly increased in *Hdac4*$^{ob-/-}$ without PTH treatment compared with *Hdac4*$^{fl/fl}$ mice (Fig. 6D) and remained elevated with PTH treatment. Utilizing real time RT-qPCR, we observed that the expression levels of *Mmp13* were higher in the PTH-treated wild-type

mice than in the vehicle control (Fig. 6E). In *Hdac4*$^{ob-/-}$ mice, the expression tended to increase compared with vehicle-treated mice but did not achieve statistical significance. Interestingly, *Mmp13* gene expression was lower in PTH-treated *Hdac4*$^{ob-/-}$ mice compared to PTH-treated *Hdac4*$^{fl/fl}$ mice. These results suggest that HDAC4 counteracts both basal and PTH-induced bone resorption. Nevertheless, HDAC4 is necessary for inducing *Mmp13* gene expression by continuous PTH. It should be noted that *RankL* and *Opg* mRNA levels were not significantly different across the groups at the time the mice were killed.

HDAC4 exerts an anabolic effect

Next, to determine the role of HDAC4 in possible anabolic effects on bone, we investigated biomarkers of bone formation: serum P1NP and *Col1a1* (Type I collagen) mRNA levels. As shown in Fig.7A, PTH-treated mice responded with a significant increase in serum P1NP levels compared to vehicle controls. Next, we observed *Col1a1* was increased in the PTH-treated mice (Fig.7B). On the other hand, in *Hdac4*$^{ob-/-}$ mice, serum P1NP and *Col1a1* (Type I collagen) levels were not changed compared to *Hdac4*$^{fl/fl}$ mice (Fig. 7A, B). Runx2 is an essential regulator for osteoblastic function, and regulates many osteoblastic genes, including *Col1a1 and Mmp13*.[18, 19] Interestingly, *Runx2* expression did not change in *Hdac4*$^{ob-/-}$ mice, however it was decreased in the PTH-treated *Hdac4*$^{ob-/-}$ mice (Fig.7C). Osterix (OSX) acts downstream of RUNX2 during bone development, and interacts with RUNX2 to coordinately induce the expression of the *Col1a1* gene.[20] Fig 7D demonstrated that *Osx* expression has a similar pattern to *Runx2* although the differences were not significant. These results suggest that HDAC4 is required to maintain *Runx2* expression after continuous PTH treatment. RUNX2 and OSX have been shown to regulate the *SOST* promoter in human cells.[21]

Continuous PTH treatment did not affect *Sost* mRNA levels in the *Hdac4*$^{fl/fl}$ mice (Fig 8a). In contrast, *Sost* mRNA was highly elevated in *Hdac4*$^{ob-/-}$ mice compared with *Hdac4*$^{fl/fl}$ mice. Surprisingly, deletion of HDAC4 in osteoblast lineage cells resulted in a significant inhibition of *Sost* expression by PTH. Sclerostin, a protein encoded by the *Sost* gene and expressed by osteocytes, inhibits osteoblastic bone formation.[12, 21] To confirm protein levels of sclerostin, we performed immunohistochemistry (IHC) and found that staining for sclerostin was stronger and the percentage of sclerostin-ositive osteocytes in *Hdac4*$^{ob-/-}$ mice was increased compared to *Hdac4*$^{fl/fl}$ mice and in these mice, PTH treatment caused a decrease in sclerostin staining (Fig. 8B, C). These results indicate that HDAC4 has an anabolic effect, likely at least in part via inhibition of *Sost* mRNA and sclerostin protein levels, and this is attenuated by continuous PTH in the absence of HDAC4. Since we have found that HDAC4 and HDAC5 co-immunoprecipitate (data not shown) and have been shown to co-regulate *Sost* in osteocytic cells[15], we analyzed *Hdac5* expression but it did not change in *Hdac4*$^{ob-/-}$ mice with and without PTH (Fig. 8D).

Discussion

Here, we describe the conditional deletion of *Hdac4* by using the *Cre-loxP* system to analyze the function of HDAC4 in differentiated mature osteoblasts and osteocytes and its role in PTH's catabolic action on bone. Both continuous and intermittent PTH increase bone

turnover in trabecular and cortical bones. However, chronic PTH elevation is associated with excess production of osteoclasts coupled to increased osteoblasts with a negative balance between bone formation and resorption, consequently resulting in a final net bone loss. Primary hyperparathyroidism and continuous PTH treatment cause cortical bone loss by enhancing endosteal resorption through stimulation of osteoclast formation and activity.[23, 24] PTH also stimulates both the resorption and the formation of trabecular bone[24, 25, 26, 27] and severe chronic elevation of PTH levels may lead to trabecular bone loss.[24] In agreement with previous studies, our data showed that continuous PTH induced both cortical and trabecular bone loss, and increased osteoclast number and activity but continuous PTH also stimulated bone formation markers, serum P1NP levels and Type I collagen mRNA.

Our μCT analyses showed that *Hdac4*$^{ob-/-}$ mice have significantly reduced cortical thickness and bone area, and no difference was seen in trabecular bone. Cortical bone, which represents more than 80% of skeletal mass, provides important mechanical support.[28, 29] Bone growth in width is achieved through periosteal apposition from the action of periosteal osteoblasts[30], and resorption at the endosteal surface. [31] The balance between periosteal bone apposition and endosteal bone resorption is important for advancing bone growth; producing greater cortical bone diameter and thickness. We suggest that HDAC4 in mature osteoblasts plays an important role in the maintenance of cortical bone. Interestingly, *Hdac4*$^{ob-/-}$ mice showed attenuated PTH catabolic actions in cortical bone, but not in trabecular bone. Elevated PTH levels in humans are associated with a lower bone mass at all skeletal sites, but particularly at sites containing predominantly cortical bone.[32] In fact, both hyperparathyroidism and continuous PTH treatment usually produce a modest increase in trabecular bone.[27, 33]

The findings described in this report demonstrate that HDAC4 in mature osteoblasts functions as a repressor of basal bone resorption but is required for the bone resorptive effects of continuous PTH. We also showed that HDAC4 contributes to blocking the antianabolic effect of *Sost*/sclerostin expression; on the other hand, continuous PTH is able to decrease *Sost*/sclerostin expression in the absence of HDAC4. It has been shown that *Sost* transcription is controlled mainly via its proximal promoter and distal enhancer (evolutionarily conserved region 5, ECR5).[34] RUNX2 and osterix (OSX) bind to the *SOST* promoter and have been shown to positively regulate *SOST* expression in human cells.[21] The distal enhancer, ECR5, is a 255-bp fragment within the 52kb VB region of the *Sost* gene. It has been shown that ECR5 is essential for *Sost* expression in mouse osteocytes[35] and Mef2c is involved in both basal and PTH-decreased *Sost* expression through the MEF2 binding site within the ECR5 element.[17, 35] Wein *et al.* have shown that HDAC5 binds to the *Sost* enhancer and inhibits the function of Mef2c in osteocytes.[15] The same researchers have reported that HDAC4/5 are required for PTH repression of *Sost* through effects on Mef2c binding to the *Sost* enhancer in osteocytes.[36] They showed that *Sost* mRNA was increased in mice lacking *Hdac5*, but not in mice with *Hdac4* deletion from osteocytes using DMP1-Cre, but deletion of both *Hdac4* and *Hdac5* showed a greater increase than *Hdac5* single knockout. The double knockout mice showed abolition of PTH-induced *Sost*-regulation. In addition, Baertschi et al. have shown that PTH leads to a rapid and strong nuclear localization of HDAC5 and an increase in nuclear HDAC4 in UMR 106 cells.[16]

The decrease in *Sost* mRNA after PTH treatment in the *Hdac4*$^{ob-/-}$ mice may be due to unimpeded translocation of HDAC5 into nuclei which does not appear to occur in the wild type mice. Here, we showed that *Sost*/sclerostin expression was increased in mice with *Hdac4* deletion from mature osteoblasts and this was attenuated by continuous PTH.

Col2.3-Cre is known to be active in the mature osteoblast lineage (osteoblasts and osteocytes).[37] Mef2c and sclerostin co-localize in osteoblastic cells, UMR 106 cells, and mouse osteocytes.[17] It has been reported that the *SOST* promoter is required for high levels of osteocyte specific expression, although ECR5 is sufficient to induce expression in osteocytes.[35] It seems that both promoter and enhancer are necessary for *Sost* gene regulation. Previously we reported in UMR 106–01 cells that, for the *Mmp13* promoter, Runx2 associates with the RD site and c-Fos and c-Jun together with Mef2c associate with the AP-1 site. Under basal conditions, HDAC4 inhibits *Mmp13* expression through interaction with Runx2, and PTH induces *Mmp13* transcription by regulating the dissociation of HDAC4 from Runx2.[8, 38] HDAC5, Runx2 and Mef2c may be involved in the regulation of *Sost* expression in *Hdac4*$^{ob-/-}$ mice although *Hdac5* and *Mef2c* expression did not significantly change in the *Hdac4*$^{ob-/-}$ mice with and without PTH. Notably, Runx2 expression was decreased in the *Hdac4*$^{ob-/-}$ mice after continuous PTH treatment suggesting that HDAC4 is required for maintaining Runx2 expression under these conditions. One reason for the decrease in *Sost*/sclerostin expression, and the lesser increase in *Mmp13*, in PTH-treated *Hdac4*$^{ob-/-}$ mice may be due to the reduction in Runx2.

Previous reports showed that *Sost*/sclerostin expression is suppressed by PTH.[13, 14, 17, 39] Our results demonstrate no suppression of *Sost*/sclerostin expression after continuous PTH treatment in wild-type mice. Perhaps this difference is due to the dose and duration of PTH. Many studies have observed this effect with anabolic PTH injections or in vitro. Others have shown suppression of *Sost*/sclerostin expression in rodent models with catabolic treatment with PTH (continuous treatment)[13, 14], but they examined acute effects of PTH. We used 80μg/kg/d for 14 days, whereas these studies used 1.5–7.5 times higher doses of PTH and *Sost*/sclerostin expression was examined 90 min, 4 hours or 24–96 hours after PTH treatment, while we examined expression at the end of the experiment after 14 days. Actually, it has been reported that intermittent PTH decreased *Sost* mRNA levels but the effect was transient.[13, 14] Intermittent PTH did not significantly affect *Sost* expression or sclerostin protein after 4 days. Continuous PTH decreased *Sost* expression around 40 h and after that, it tended to return to original levels.[14]

We found an interesting observation that mice lacking *Hdac4* in mature osteoblasts had a shorter tail due to shorter caudal vertebrae (without affecting the caudal vertebrae numbers), with almost no growth plate, and caudal vertebral cortical bone mass and strength were decreased in *Hdac4*$^{ob-/-}$ mice. Interestingly, the phenotype of the tail takes place after 7 postnatal days (data not shown), suggesting it is due to postnatal, not embryologic development. This is the period when caudal vertebrae undergo endochondral ossification[40], so the transition to bone may be responsible for the aberrant intervertebral discs. Our data indicate that HDAC4 in the mature osteoblast lineage is necessary for the correct proliferation and differentiation of chondrocytes in the caudal vertebrae, and the effect is more severe than in lumbar vertebrae or long bones (data not shown). Further

studies are needed to better understand the function of HDAC4 in the mature osteoblast lineage for caudal vertebrae and development of the intervertebral disc.

In conclusion, the results of the present report demonstrate that HDAC4 in the mature osteoblast lineage influences cortical bone mass and thickness and is necessary for the catabolic effect of PTH in cortical bone. HDAC4 inhibits bone resorption and also may have an anabolic effect via inhibiting *Sost*/sclerostin expression (Fig. 9).

Supplementary Material

Refer to Web version on PubMed Central for supplementary material.

Acknowledgements:

We thank Dr. Eric Olson for kindly giving us the HDAC4 floxed mice (*Hdac4*$^{fl/fl}$). We thank Dr. Malvin Janal for advice on statistical analyses.

Financial support:

This work was supported by NIH grant R01DK4720 to Dr. Nicola C. Partridge.

REFERENCES

1. Silva BC, Costa AG, Cusano NE, Kousteni S, Bilezikian JP. Catabolic and anabolic actions of parathyroid hormone on the skeleton. J Endocrinol Invest 2011;34:801–10. [PubMed: 21946081]
2. Zhao W, Byrne MH, Boyce BF, Krane SM. Bone resorption induced by parathyroid hormone is strikingly diminished in collagenase-resistant mutant mice. J Clin Invest 1999;103:517–24 [PubMed: 10021460]
3. McGee-Lawrence ME, Westendorf JJ. Histone deacetylases in skeletal development and bone mass maintenance. Gene 2011;474:1–11. [PubMed: 21185361]
4. Vega RB, Matsuda K, Oh J, Barbosa AC, Yang X, Meadows E, McAnally J, Pomajzl C, Shelton J, Richardson JA, Karsenty G, and Olson EN. Histone deacetylase 4 controls chondrocyte hypertrophy during skeletogenesis. Cell 2004;119: 555–66. [PubMed: 15537544]
5. Arnold MA,Yim K, Czubryt MP, Phan D, McAnally J, Qi X, Shelton JM, Richardson JA,, Bassel-Duby R, and Olson EN. MEF2C transcription factor controls chondrocyte hypertrophy and bone development. Dev Cell 2007;12:377–89. [PubMed: 17336904]
6. Jeon EJ, Lee KY, Coi NS, Jin YH, Ryoo HM, Choi JY, Yoshida M, Nishino N, Oh BC, Lee KS, LeeYH, Bae SC. Bone morphogenetic protein-2 stimulates Runx2 acetylation. J Biol Chem 2006;281:16502–11. [PubMed: 16613856]
7. Nakatani T, Chen T, Partridge NC. MMP-13 is one of the critical mediators of the effect of HDAC4 deletion on the skeleton. Bone 2016;90:142–51. [PubMed: 27320207]
8. Shimizu E, Selvamurugan N, Westendorf JJ, Olson EN, Partridge NC. HDAC4 represses matrix metalloproteinase-13 transcription in osteoblastic cells, and parathyroid hormone controls this repression. J Biol Chem 2010;285:9616–26. [PubMed: 20097749]
9. Nakatani T, Partridge NC. MEF2C interacts with c-FOS in PTH-stimulated Mmp13 gene expression in osteoblastic cells. Endocrinology 2017;158:3778–91. [PubMed: 28973134]
10. Obri A, Makinistoglu MP, Zhang H, Karsenty G. HDAC4 integrates PTH and sympathetic signaling in osteoblasts. J Cell Biol 2014; 205:771–80. [PubMed: 24934156]
11. Winkler DG, Sutherland MK, Geoghegan JC, Yu C, Hayes T, Skonier JE, Shpektor D, M Jonas M, Kovacevich BR, Staehling-Hampton K, Appleby M, Brunkow ME, Latham JA. Osteocyte control of bone formation via sclerostin, a novel BMP antagonist. EMBO J 2003;22:6267–76. [PubMed: 14633986]

12. van Bezooijen RL, Roelen BA, Visser A, van der Wee-Pals L, de Wilt E, Karperien M, Hamersma H, Papapoulos SE, ten Dijke P, Löwik CW. Sclerostin is an osteocyte-expressed negative regulator of bone formation, but not a classical BMP antagonist. J Exp Med 2004;199:805–14. [PubMed: 15024046]
13. Keller H, Kneissel M. SOST is a target gene for PTH in bone. Bone 2005;37:148–58. [PubMed: 15946907]
14. Bellido T, Ali AA, Gubrij I, Plotkin LI, Fu Q, O'Brien CA, Manolagas SC, Jilka RL. Chronic elevation of parathyroid hormone in mice reduces expression of sclerostin by osteocytes: a novel mechanism for hormonal control of osteoblastogenesis. Endocrinology 2005;146:4577–83. [PubMed: 16081646]
15. Wein MN, Spatz J, Nishimori S, Doench J, Root D, Babij P, Nagano K, Baron R, Brooks D, Bouxsein M, Pajevic PD, Kronenberg HM. HDAC5 controls MEF2C-driven sclerostin expression in osteocytes. J Bone Miner Res 2015;30:400–11. [PubMed: 25271055]
16. Baertschi S, Baur N, Lueders-Lefevre V, Voshol J, Keller H. Class I and IIa histone deacetylases have opposite effects on sclerostin gene regulation. J Biol Chem 2014;289:24995–5009. [PubMed: 25012661]
17. Leupin O, Kramer I, Collette NM, Loots GG, Natt F, Kneissel M, Keller H. Control of the SOST bone enhancer by PTH using MEF2 transcription factors. J Bone Miner Res. 2007;22:1957–67. [PubMed: 17696759]
18. Kern B, Shen J, Sterbuck M, and Karsenty G. Cbfa1 contributes to the osteoblast-specific expression of type I collagen genes. J. Biol. Chem 2001;276:7101–07. [PubMed: 11106645]
19. Selvamurugan N, Jefcoat SC, Kwok S, Kowalewski R, Tamasi JA, Partridge NC. Overexpression of Runx2 directed by the matrix metalloproteinase-13 promoter containing the AP-1 and Runx/RD/Cbfa sites alters bone remodeling in vivo. J. Cell Biochem 2006;99:545–57. [PubMed: 16639721]
20. Ortuño MJ, Susperregui A, Artigas N, Rosa JL, Ventura F. Osterix induces Col1a1 gene expression through binding to Sp1 sites in the bone enhancer and proximal promoter regions. Bone 2013;52:548–56. [PubMed: 23159876]
21. Pérez-Campo FM, Santurtún A, García-Ibarbia C, Pascual MA, Valero C, Garcés C, Sañudo C, Zarrabeitia MT, Riancho JA. Osterix and RUNX2 are transcriptional regulators of sclerostin in human bone. Calcif Tissue Int 2016;99:302–9. [PubMed: 27154028]
22. Poole KE, Reeve J. Parathyroid hormone - a bone anabolic and catabolic agent. Curr Opin Pharmacol 2005;5:612–7. [PubMed: 16181808]
23. Lotinun S, Evans GL, Bronk JT, Bolander ME, Wronski TJ, Ritman EL, Turner RT. Continuous parathyroid hormone induces cortical porosity in the rat: effects on bone turnover and mechanical properties. J Bone Miner Res 2004;19:1165–71. [PubMed: 15177000]
24. Iida-Klein A, Lu SS, Kapadia R, Burkhart M, Moreno A, Dempster DW, Lindsay R. Short-term continuous infusion of human parathyroid hormone 1–34 fragment is catabolic with decreased trabecular connectivity density accompanied by hypercalcemia in C57BL/J6 mice. J Endocrinol 2005;186:549–57. [PubMed: 16135674]
25. Dempster DW, Parisien M, Silverberg SJ, Liang XG, Schnitzer M, Shen V, Shane E, Kimmel DB, Recker R, Lindsay R, Bilezikian JP. On the mechanism of cancellous bone preservation in postmenopausal women with mild primary hyperparathyroidism. J Clin Endocrinol Metab 1999;84:1562–66. [PubMed: 10323380]
26. Qin L, Raggatt LJ, Partridge NC. Parathyroid hormone: a double-edged sword for bone metabolism. Trends Endocrinol Metab 2004;15:60–5. [PubMed: 15036251]
27. Zhou H, Shen V, Dempster DW, Lindsay R. Continuous parathyroid hormone and estrogen administration increases vertebral cancellous bone volume and cortical width in the estrogen-deficient rat. J Bone Miner Res 2001;16:1300–7. [PubMed: 11450706]
28. Zebaze RM, Ghasem-Zadeh A, Bohte A, Iuliano-Burns S, Mirams M, Price RI, Mackie EJ, Seeman E. Intracortical remodelling and porosity in the distal radius and post-mortem femurs of women: a cross-sectional study. Lancet 2010;375:1729–36. [PubMed: 20472174]
29. Seeman E Periosteal bone formation — a neglected determinant of bone strength. N Engl J Med 2003;349:320–23. [PubMed: 12878736]

30. Rauch F Bone growth in length and width: The Yin and Yang of bone stability. J Musculoskelet Neuronal Interact 2005;5:194–201. [PubMed: 16172510]

31. Seeman E Structural basis of growth-related gain and age-related loss of bone strength. Rheumatology 2008;47:iv2–iv8. [PubMed: 18556646]

32. Wishart J, Horowitz M, Need A, Nordin BE. Relationship between forearm and vertebral mineral density in postmenopausal women with primary hyperparathyroidism. Arch. Intern. Med 1990;150:1329–31. [PubMed: 2353865]

33. Parisien M Silverberg SJ, Shane E, de la Cruz L, Lindsay R, Bilezikian JP, Dempster DW. The histomorphometry of bone in primary hyperparathyroidism: preservation of cancellous bone structure. J. Clin. Endocrinol. Metab 1990;70:930–8. [PubMed: 2318948]

34. Loots GG, Kneissel M, Keller H, Baptist M, Chang J, Collette NM, Ovcharenko D, Plajzer-Frick I, and Rubin EM. Genomic deletion of a long-range bone enhancer misregulates sclerostin in Van Buchem disease. Genome Res 2005;15:928–35. [PubMed: 15965026]

35. Collette NM, Genetos DC, Economides AN, Xie L, Shahnazari M, Yao W, Lane NE, Harland RM, Loots GG. Targeted deletion of Sost distal enhancer increases bone formation and bone mass. Proc Natl Acad Sci U S A 2012;109:14092–7. [PubMed: 22886088]

36. Wein MN, Liang Y, Goransson O, Sunberg TB, Wang J, Williams EA, O'Meara MJ, Govea N, Beqo B, Nishimori S, Nagano K, Brooks DJ, Martins JS, Corbin B, Anselmo A, Sadreyev R, Wu JY, Sakamoto K, Foretz M, Xavier RJ, Baron R, Bouxsein ML, Gardella TJ, Divieti-Pajevic P, Gray NS, Kronenberg HM. SIKs control osteocyte responses to parathyroid hormone. Nat Commun 2016 10 19;7:13176. doi: 10.1038/ncomms13176. [PubMed: 27759007]

37. Liu F, Woitge HW, Braut A, Kronenberg MS, Lichtler AC, Mina M, Kream BE. Expression and activity of osteoblast-targeted Cre recombinase transgenes in murine skeletal tissues. Int. J. Dev. Biol 2004;48:645–53. [PubMed: 15470637]

38. Selvamurugan N, Chou WY, Pearman AT, Pulumati MR, Partridge NC. Parathyroid hormone regulates the rat collagenase-3 promoter in osteoblastic cells through the cooperative interaction of the activator protein-1 site and the runt domain binding sequence. J Biol Chem 1998;273:10647–57. [PubMed: 9553127]

39. Bellido T, Saini V, Pajevic PD. Effects of PTH on osteocyte function. Bone 2013;54:250–7. [PubMed: 23017659]

40. Hankenson FC, Garzel LM, Fischer DD, Nolan B, Hankenson KD. Evaluation of tail biopsy collection in laboratory mice (Mus musculus): vertebral ossification, DNA quantity, and acute behavioral responses. J Am Assoc Lab Anim Sci 2008;28:10–18.

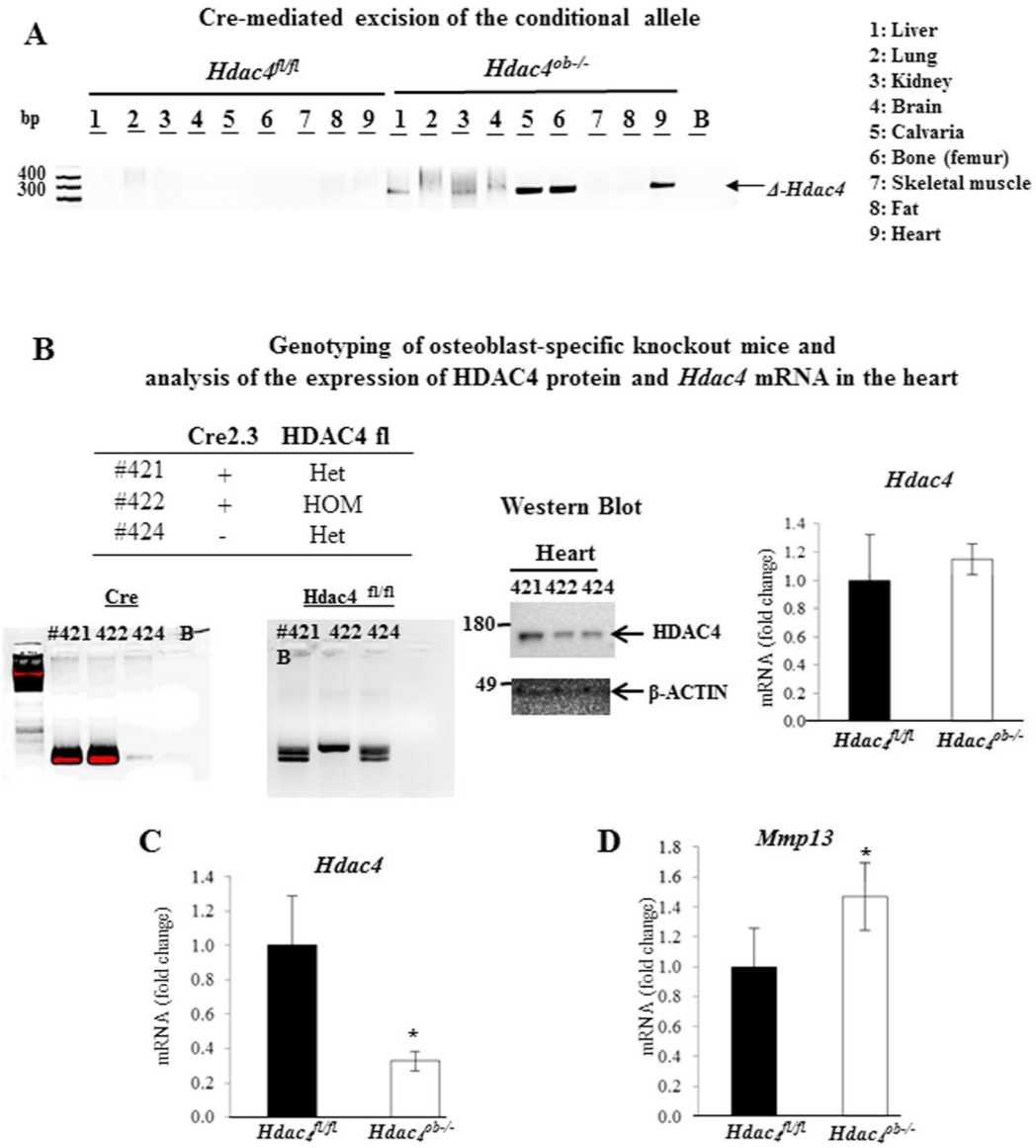

Figure:1.

(A) Detection of the deletion allele of *Hdac4* by PCR in genomic DNA isolated from different tissues using primers arm1 and arm3. (B) Genotyping of Hdac4 mice using primers arm1 and arm2. Analysis of the expression of HDAC4 protein and *Hdac4* mRNA in the heart. β-actin was used as a loading control. (C) *Hdac4*, and (D) *Mmp13* levels relative to β-actin were determined in distal femur RNA from 10 week-old $Hdac4^{fl/fl}$ (n = 6) and $Hdac4^{ob-/-}$ mice (n = 8). Data are shown as fold changes compared with levels in $Hdac4^{fl/fl}$ mice. Data shown are means ± SE. *, $p < 0.05$ by Student's *t* test.

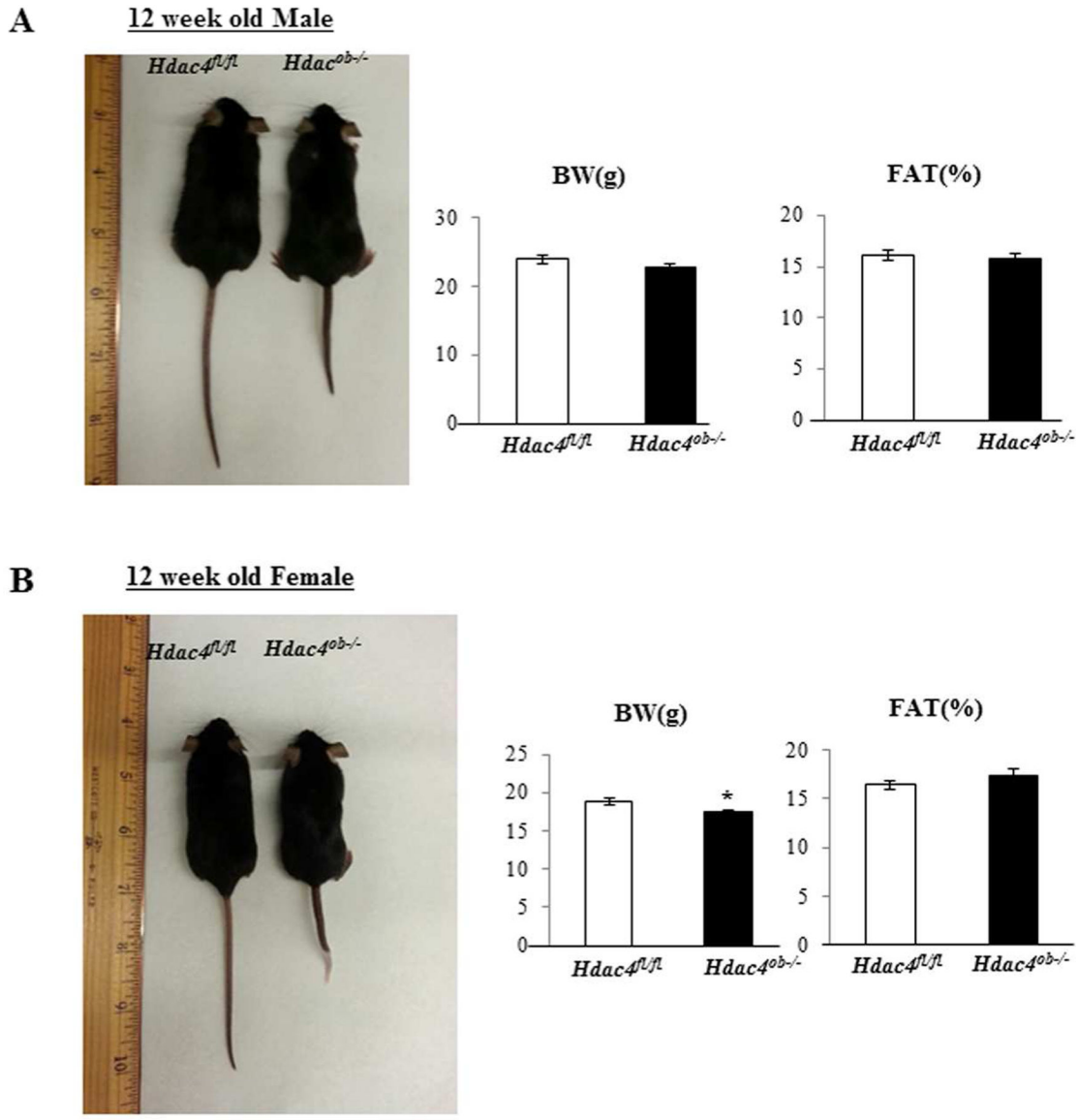

Figure. 2. Phenotype of *Hdac4*$^{ob-/-}$ compared with *Hdac4*$^{fl/fl}$ mice Twelve-week-old

(A) Male, (B) Female *Hdac4* $^{fl/fl}$ and *Hdac4*$^{ob-/-}$ mice are shown. Fat percentage was obtained by DXA scan analyses. *Hdac4* $^{fl/fl}$ (n=12) and *Hdac4*$^{ob-/-}$ mice (n=17).

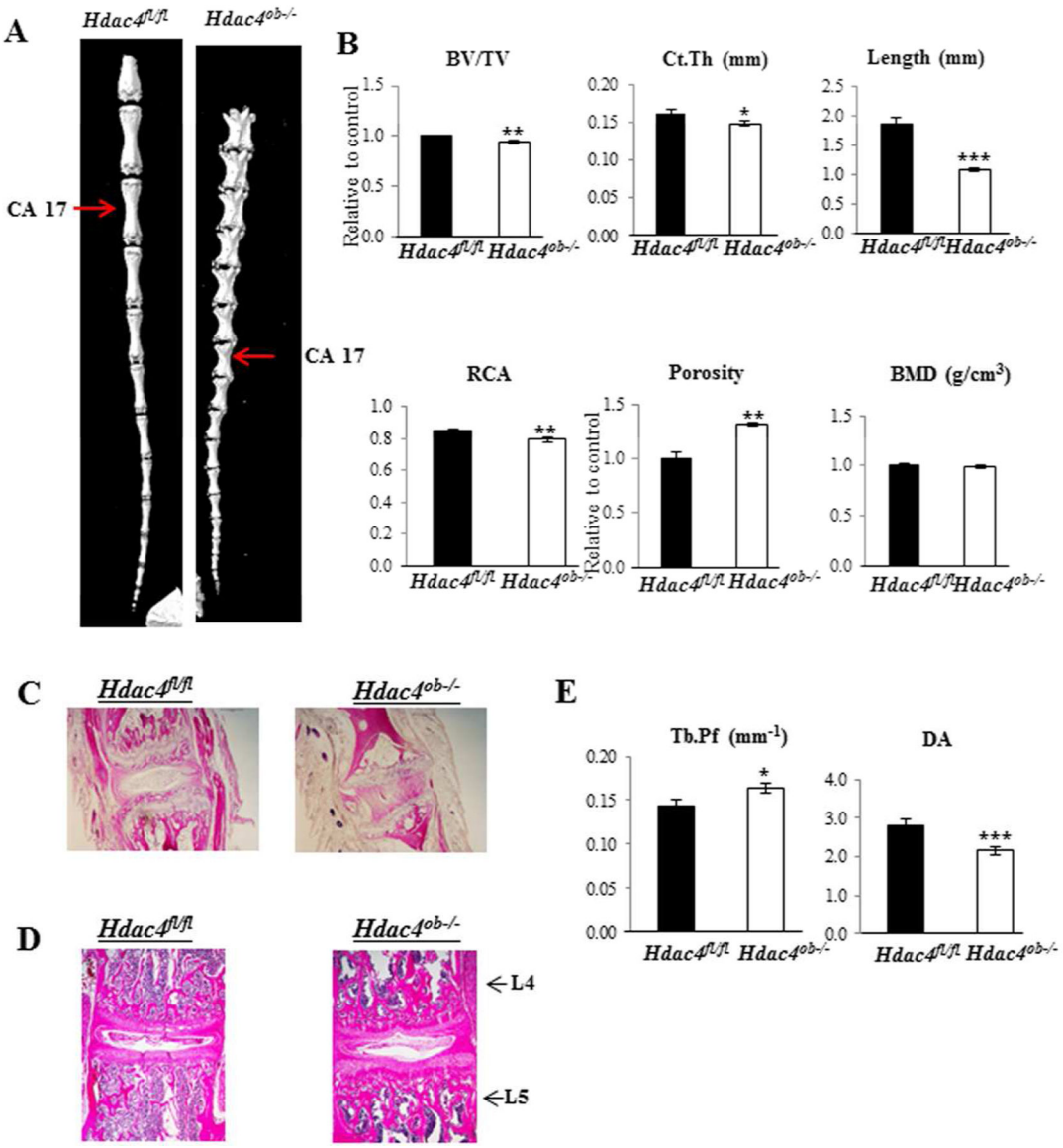

Figure 3. *Hdac4*$^{ob-/-}$ mice have decreased caudal bone mass and length compared with Hdac4$^{fl/fl}$ mice

(A) Representative uCT images of the tails are shown. (B) Caudal vertebrae (caudal 17) from 12-week-old female *Hdac4*$^{fl/fl}$ (n = 6) and *Hdac4*$^{ob-/-}$ mice (n = 8) were used for μCT analysis. Data shown are means ± SE. *, p< 0.05, **, p< 0.01, ***, p< 0.001 by Student's **t** test. Representative images of hematoxylin and eosin stained caudal (C) and lumbar vertebrae (D) are shown. (E) Lumbar vertebrae (L4) from 12-week-old female *Hdac4*$^{fl/fl}$ (n = 10) and *Hdac4*$^{ob-/-}$ mice (n = 10) were used for μCT analysis. Data shown are as means ± SE. *, p< 0.05, ***, p< 0.001 by Student's *t* test.

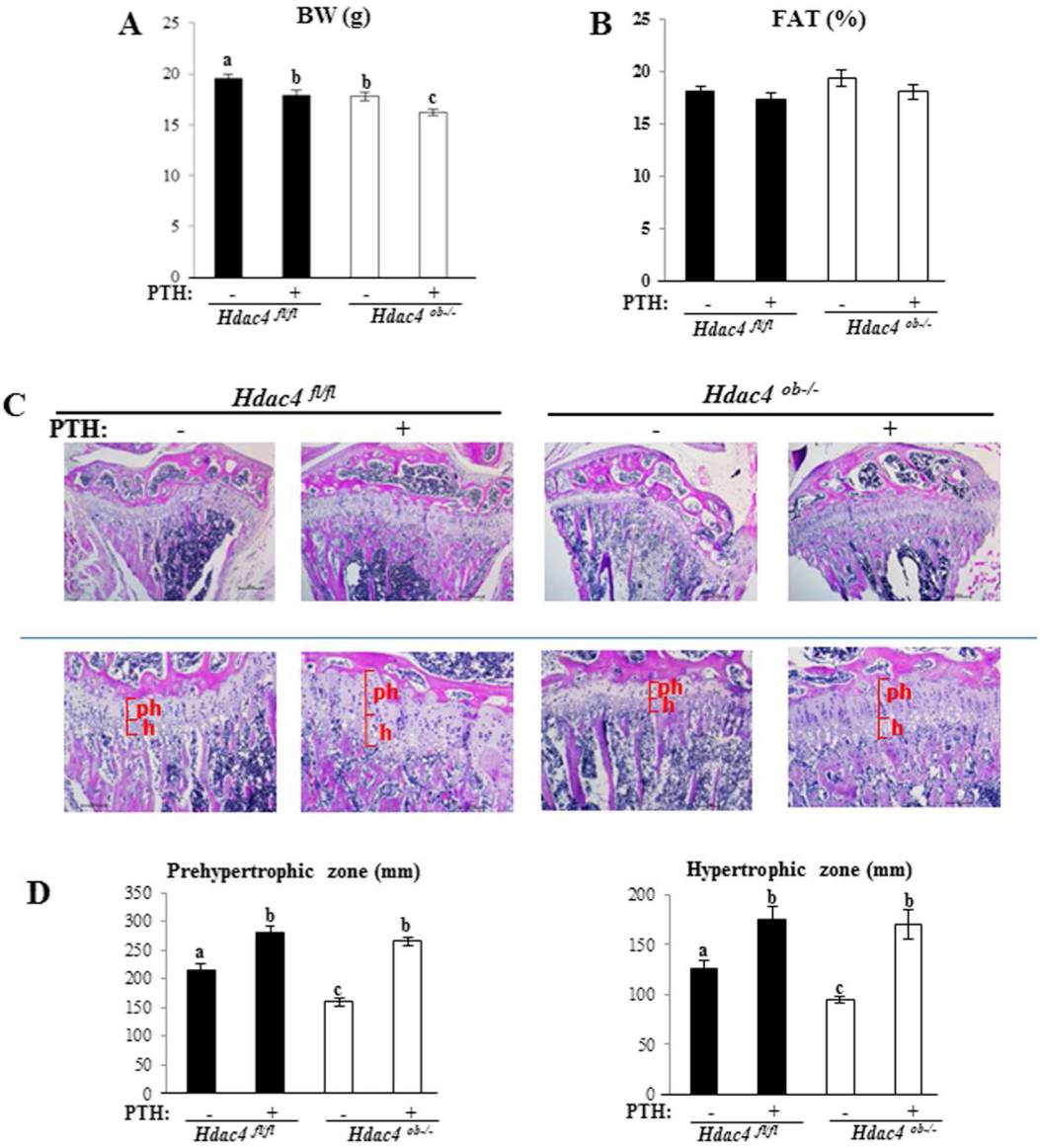

Figure 4. Body weight and growth plate histological examination of *Hdac4*$^{fl/fl}$ and *Hdac4*$^{ob-/-}$ mice after continuous PTH treatment

(A) Body weight and (B) Fat % by DXA in 10-week-old female *Hdac4*$^{fl/fl}$ and *Hdac4*$^{ob-/-}$ mice treated with continuous PTH or vehicle, (*Hdac4* $^{fl/fl}$; n=12, *Hdac4* $^{fl/fl}$ with PTH; n=13, *Hdac4*$^{ob-/-}$; n=11, *Hdac4*$^{ob-/-}$; with PTH; n=12). (C) Representative hematoxylin and eosin stained sections of the growth plate of the tibiae are shown. (D) Morphometric analysis of the length of the prehypertrophic (ph), and hypertrophic (h) zones in female mice. *Hdac4* $^{fl/fl}$; n=5, *Hdac4* $^{fl/fl}$ with PTH; n=5, *Hdac4*$^{ob-/-}$; n=6, *Hdac4*$^{ob-/-}$; with PTH; n=6. Data shown are mean ± SE. Different letters indicate $p<0.05$ vs. one another. The images were quantified using Image J software.

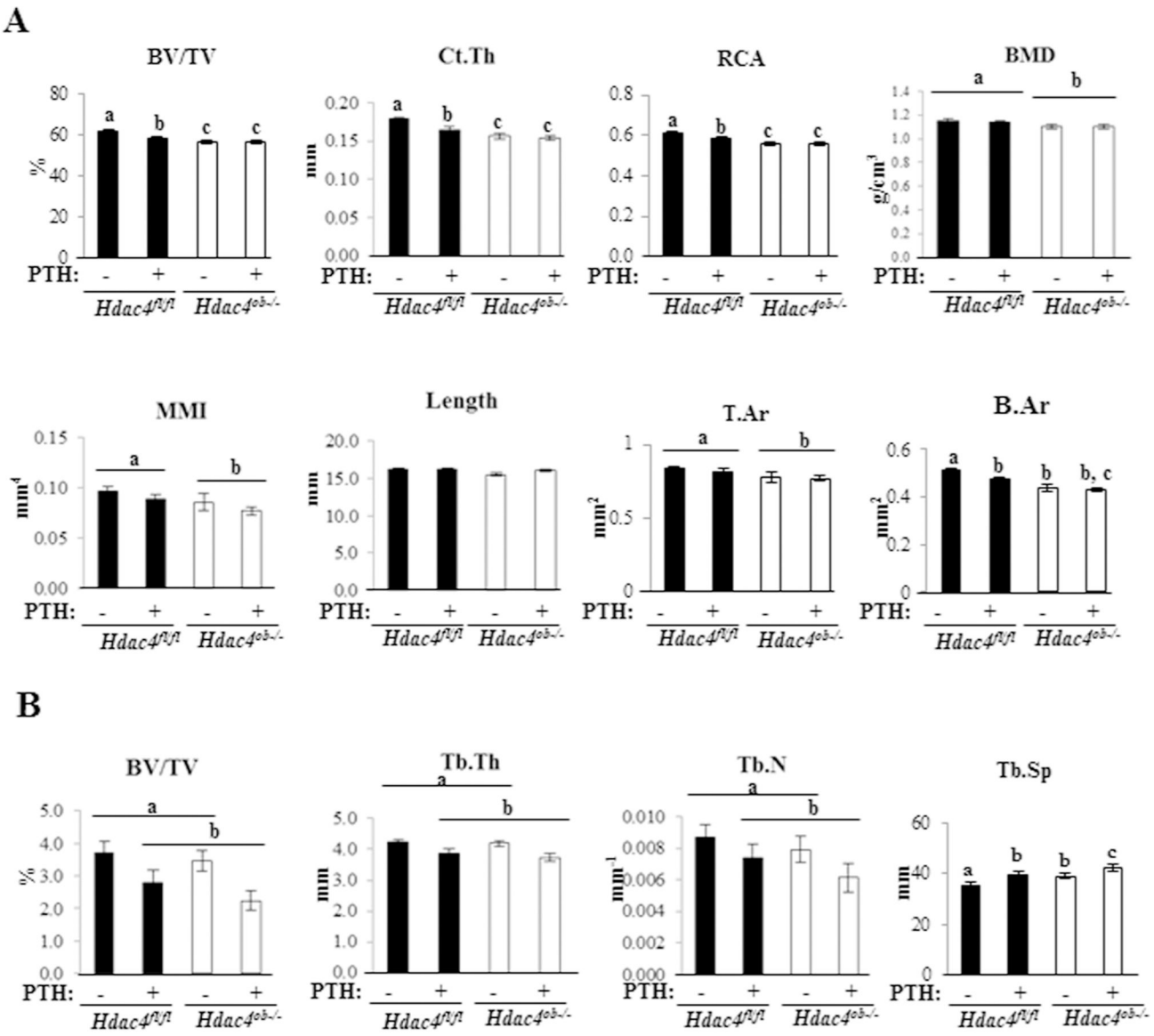

Figure 5. *Hdac4*$^{ob-/-}$ mice have decreased cortical bone but not trabecular bone and PTH is unable to cause a catabolic effect in cortical bone while this is retained in trabecular bone

(A) Tibiae from female 10-week-old female *Hdac4* $^{fl/fl}$ and *Hdac4*$^{ob-/-}$ mice treated with continuous PTH for 14 days or vehicle were used for cortical or trabecular (B) μCT analysis. (*Hdac4* $^{fl/fl}$; n=9, *Hdac4* $^{fl/fl}$ with PTH; n=11, *Hdac4*$^{ob-/-}$; n=9, *Hdac4*$^{ob-/-}$; with PTH; n=9). Data shown are means ± SE. Different letters indicate $p<0.05$ vs. one another.

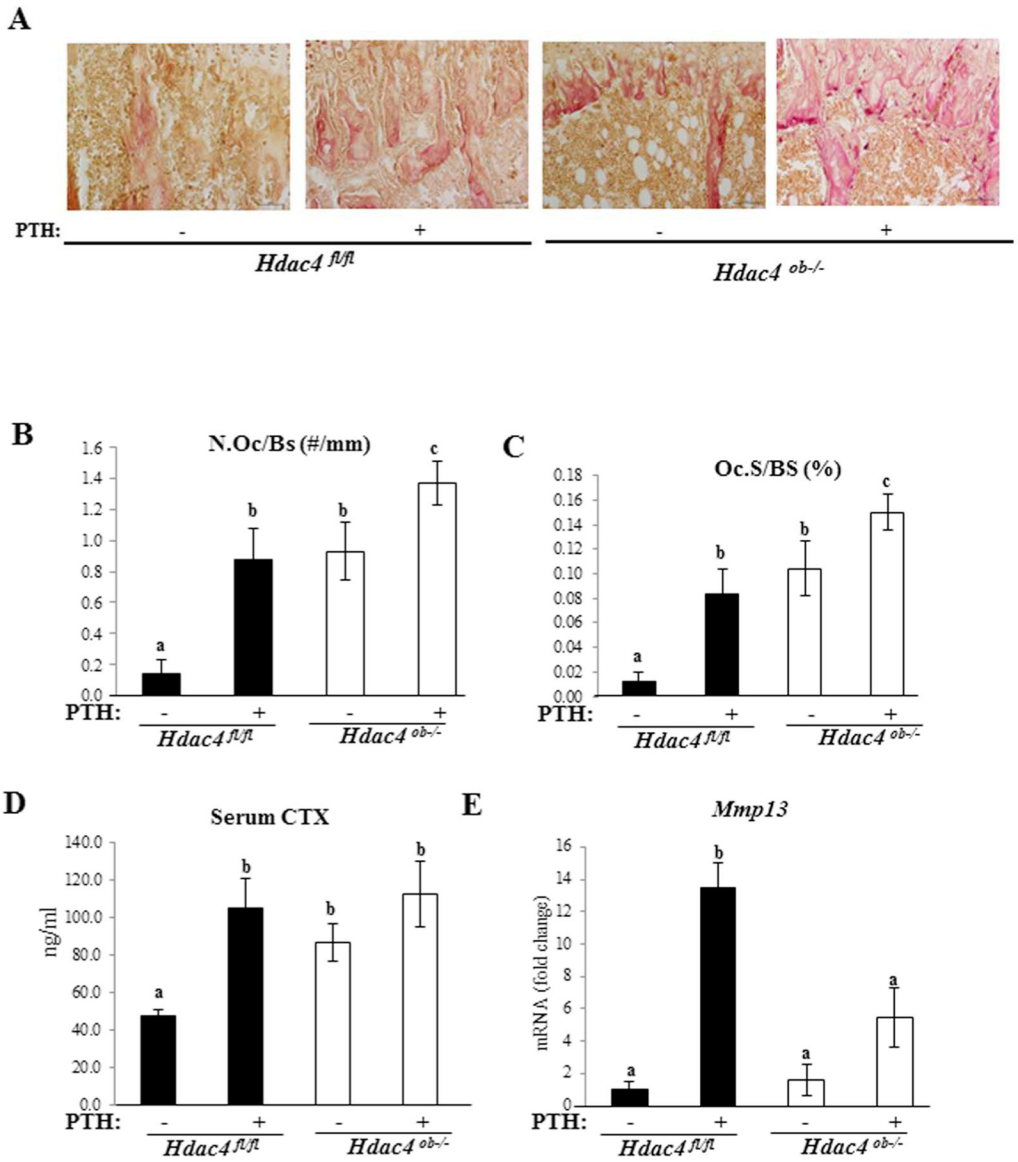

Figure 6. Osteoclast activity is increased in *Hdac4*$^{ob-/-}$ mice

(A) TRAP staining of tibiae of female 10-week-old *Hdac4*$^{fl/fl}$ and *Hdac4*$^{ob-/-}$ mice treated with PTH or vehicle is shown. 20X. (B) Quantification of osteoclast number and (C) osteoclast surface % in the animals in (A). Data shown as means ± SE. Different letters indicate $p<0.05$ vs. one another. (*Hdac4* $^{fl/fl}$; n=4, *Hdac4* $^{fl/fl}$ with PTH; n=5, *Hdac4*$^{ob-/-}$; n=−5, *Hdac4*$^{ob-/-}$; with PTH; n=4). (D) Serum CTX levels (*Hdac4* $^{fl/fl}$; n=9, *Hdac4* $^{fl/fl}$ with PTH; n=10, *Hdac4*$^{ob-/-}$; n=10, *Hdac4*$^{ob-/-}$ with PTH; n=10), data shown as means ± SE and different letters indicate $p<0.05$ vs. one another. (E) The relative levels of *Mmp13* mRNA normalized to β-actin (*Hdac4* $^{fl/fl}$; n=7, *Hdac4* $^{fl/fl}$ with PTH; n=7, *Hdac4*$^{ob-/-}$; n=6, *Hdac4*$^{ob-/-}$ with PTH; n=8). Total RNA was extracted from distal femurs of 10-week-old females and measured using real time RT-PCR. Data are shown as fold change to vehicle-treated *Hdac4*$^{fl/fl}$ and as means ± SE. Different letters indicate $p<0.05$ vs. one another.

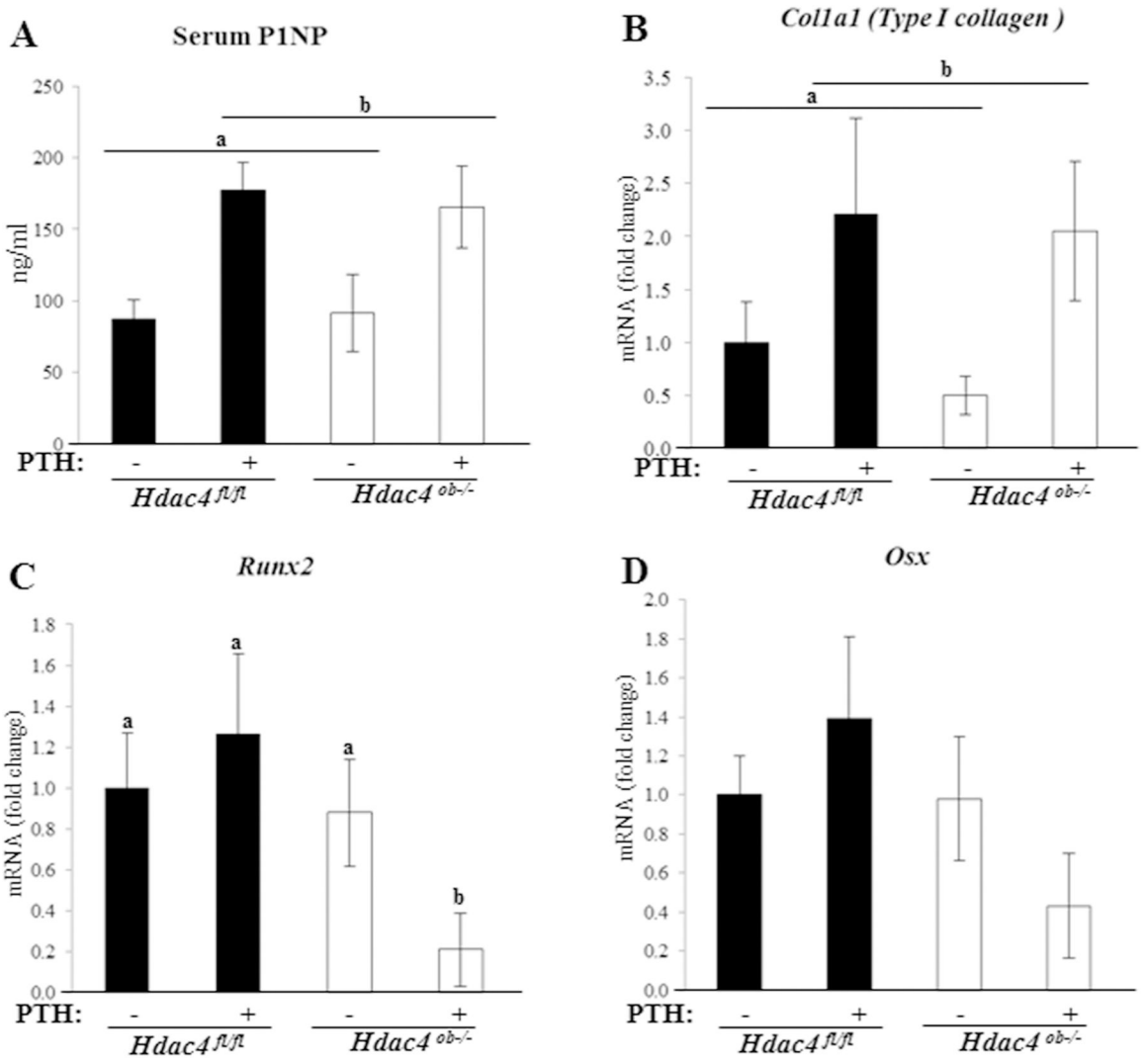

Figure 7. Bone formation markers were increased by PTH in *Hdac4* $^{fl/fl}$ and *Hdac4*$^{ob-/-}$ mice while Runx2 decreased

Ten-week-old female *Hdac4* $^{fl/fl}$ and *Hdac4* $^{ob-/-}$ mice were examined after treatment with PTH or vehicle. (A) Serum P1NP levels. n=10 in all groups. Data are shown as are means ± SE. (B) *Type I collagen* mRNA, (*Hdac4* $^{fl/fl}$; n=10, *Hdac4* $^{fl/fl}$ with PTH; n=10, *Hdac4*$^{ob-/-}$; n=10, *Hdac4*$^{ob-/-}$ with PTH; n=11), (C) Runx2 mRNA(*Hdac4*$^{fl/fl}$; n=8, *Hdac4*$^{fl/fl}$ with PTH; n=10, *Hdac4*$^{ob-/-}$; n=10, *Hdac4*$^{ob-/-}$ with PTH; n=11), (D) *Osx* mRNA(*Hdac4*$^{fl/fl}$; n=8, *Hdac4*$^{fl/fl}$ with PTH; n=10, *Hdac4*$^{ob-/-}$; n=10, *Hdac4*$^{ob-/-}$ with PTH; n=11), were measured using real time RT-PCR. The relative levels of mRNAs were normalized to β-actin. Data are shown as fold change to vehicle-treated *Hdac4*$^{fl/fl}$ and as means ± SE.

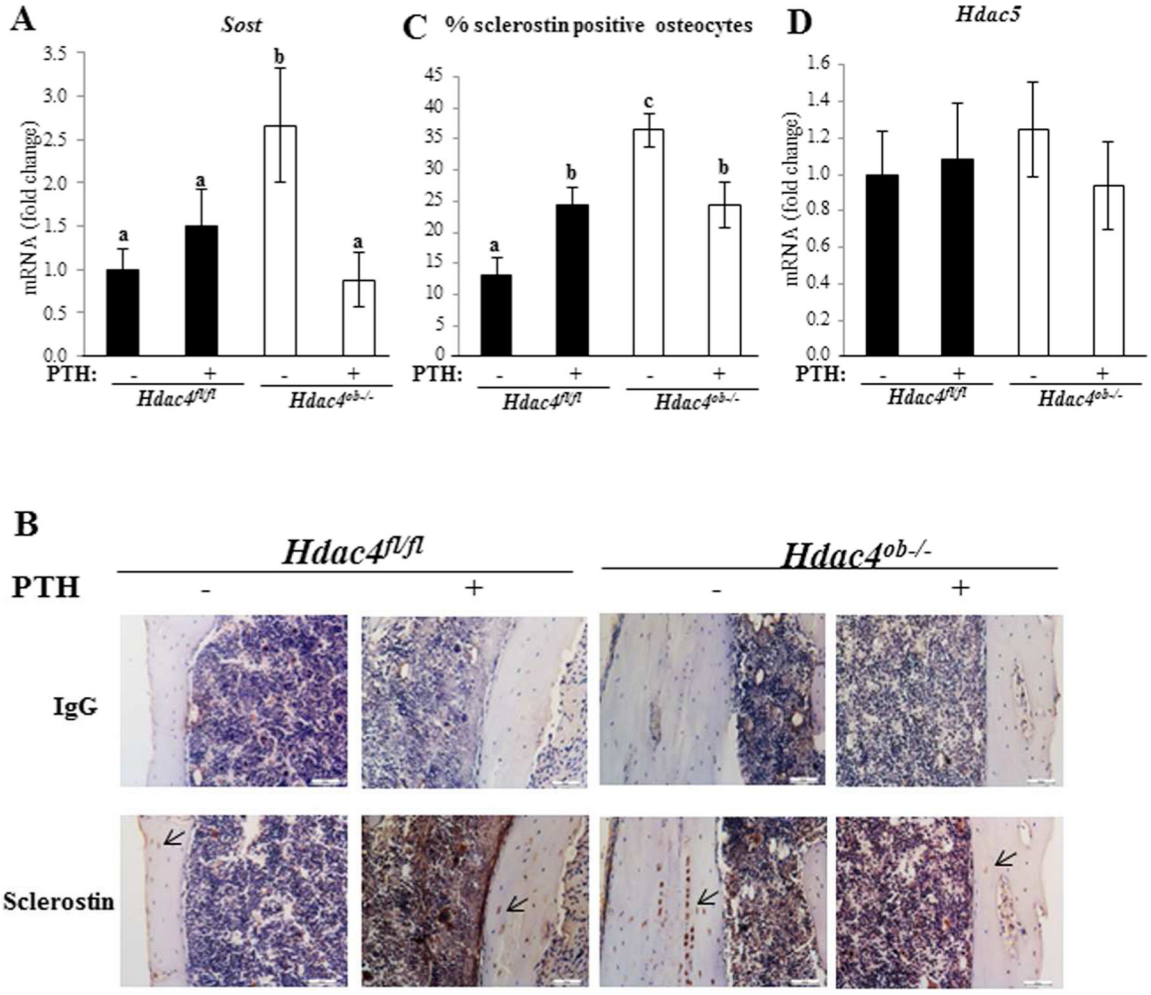

Figure 8. Increased expression of *Sost*/sclerostin in *Hdac4*$^{ob-/-}$ mice *Sost*

mRNA (A) was measured using real time RT-PCR. The relative levels of mRNAs were normalized to β-actin. Data are shown as means ± SE for –fold change to vehicle-treated *Hdac4*$^{fl/fl}$. (*Hdac4* $^{fl/fl}$; n= 9, *Hdac4* $^{fl/fl}$ with PTH; n= 9, *Hdac4*$^{ob-/-}$; n= 9, *Hdac4*$^{ob-/-}$ with PTH; n=11). (B) Immunohistochemistry for sclerostin. Representative longitudinal sections of the cortical region of the tibiae. (C) Ratio of number of sclerostin-ositive osteocytes to total number of osteocytes were quantified in lacunae of tibial cortical bones using image J (*Hdac4* $^{fl/fl}$; n=4, *Hdac4* $^{fl/fl}$ with PTH; n=4, *Hdac4*$^{ob-/-}$; n=8, *Hdac4*$^{ob-/-}$ with PTH; n=5). Data shown as means ± SE. Different letters indicate $p<0.05$ vs. one another. *Hdac5* mRNA (D) was measured using real time RT-PCR (*Hdac4* $^{fl/fl}$; n= 8, *Hdac4* $^{fl/fl}$ with PTH; n= 8, *Hdac4*$^{ob-/-}$; n= 8, *Hdac4*$^{ob-/-}$; with PTH; n=7). Data are shown as fold change to vehicle-treated *Hdac4*$^{fl/fl}$ and as means ± SE.

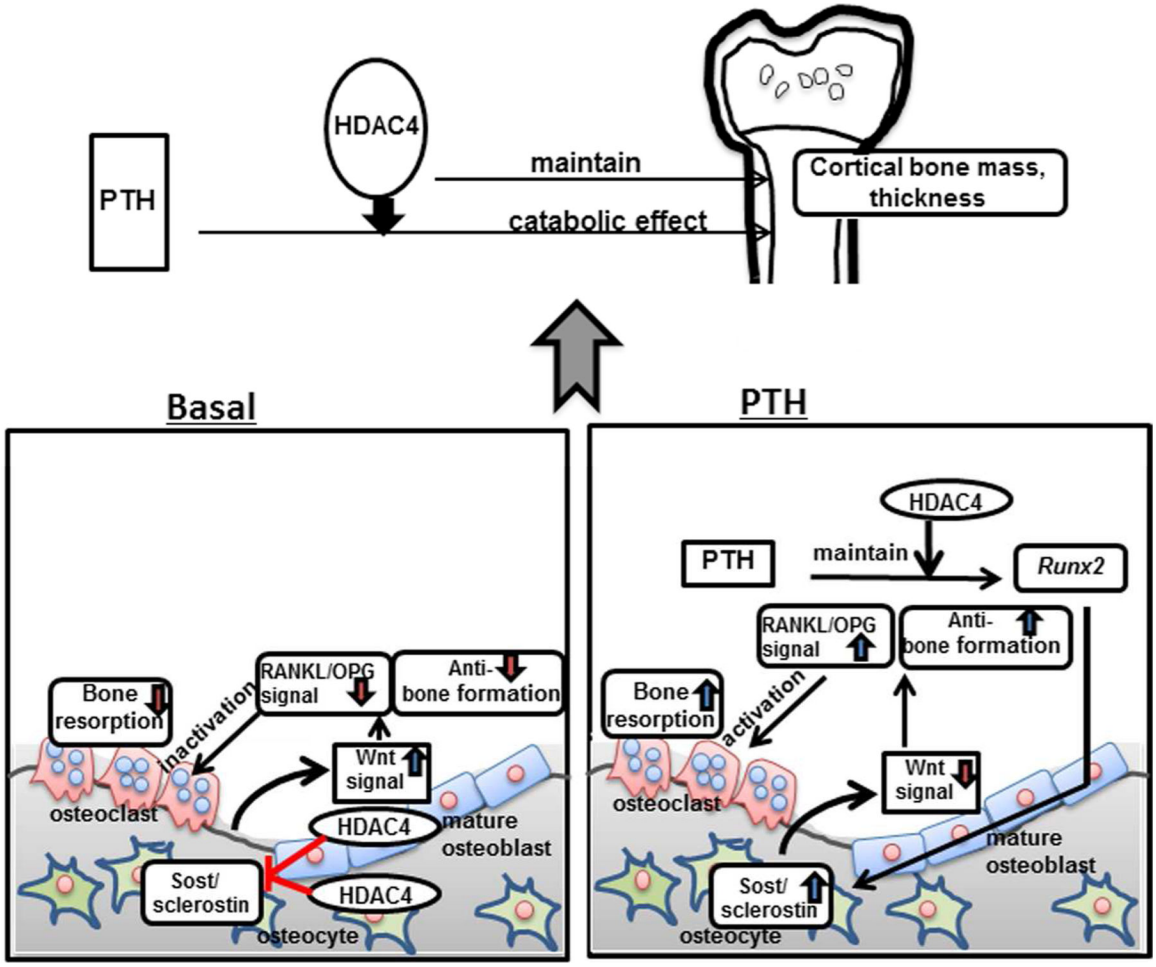

Figure 9. Proposed model depicting the functions of HDAC4 in the mature osteoblast and osteocyte

Under basal conditions, HDAC4 in mature osteoblasts and osteocytes inhibits bone resorption and also has an anabolic effect via inhibiting Sost gene and sclerostin protein expression. After continuous PTH treatment, HDAC4 is necessary for maintaining Runx2 expression. Since Runx2 contributes to Sost gene transcription, continuous PTH decreases Sost and sclerostin in the absence of HDAC4. This leads to a combined increase in bone formation and no resorptive effect of PTH in the absence of HDAC4. These actions indicate the function of HDAC4 in maintaining cortical bone mass and its role in the catabolic effects of PTH on cortical bone.

TABLE 1.

Primer sequences used in genotyping

Arm1: ATCTGCCCACCAGAGTATGTG
Arm2 : AGCTGCAGGAGTTTGTTCTCAACAAG
Arm3 : GCTGTCTTGTGGAGAATTGGAG

TABLE 2

Primer sequences for real-time RT-PCR

Gene	Primers (5'–3')
Mouse *Hdac4*	Forward, GGCGAGCACAGAGGTGAAGATG
	Reverse, GCTGTGCTGTGTCTTCCCAIAC
Mouse *Hdac5*	Forward, AAGTTGTTCGCAGATGCCCA
	Reverse, TTCACCACAGTGGGTTGGTC
Mouse *Mmpl3*	Forward, GCCCTGATGTTTCCCATCTA
	Reverse, TTTTGGGATGCTTAGGGTTG
Mouse *Collal*	Forward, AGATTGAGAACATCCGCAGCC
	Reverse, TCCAGTACTCTCCGCTCTTCC
Mouse *Sost*	Forward, AGCCTTCAGGAATGATGCCAC
	Reverse, TTTGGCGTCATAGGGATGGT
Mouse *Osx*	Forward, AGAGGTTCACTCGCTCTGACGA
	Reverse, TTGCTCAAGTGGTCGCTTCTG
Mouse *Runx2*	Forward, CCCAGCCACCTTTACCTACA
	Reverse, TATGGAGT GCT GCT GGT
Mouse *b-Actin*	Forward, TCCTCCTGAGCGCAAGTACTCT
	Reverse, CGGACTCATCGTACTCCTGCTT